Indian Journal of Chemistry
Vol. 57A, October 2018, pp. 1249-1256

Synthesis and characterization of Cu and Ag based mixed metal nanoparticle composite for antibacterial applications

Sadhucharan Mallick

Department of Chemistry, Indira Gandhi National Tribal University, Amarkantak 484 886, Anuppur, Madhya Pradesh, India

Email: sadhucharan@igntu.ac.in/ sadhu.iitd@gmail.com

Iodinated mixed metal (copper, Cu and silver, Ag) nanoparticle (NPs) composite was prepared in chitosan polymeric matrix and characterized by transmission electron microscopy (TEM), X-ray diffraction (XRD), and energy dispersive X-ray analysis (EDX). The TEM analysis demonstrated that the Cu NPs and Ag NPs had an average size of 11.4 nm and 3.4 nm, respectively. Detailed antibacterial studies have been carried out on green fluorescent protein (GFP) expressing Gram-negative *Escherichia coli* (*E. coli*) bacteria. The synergistic antibacterial effect of iodinated mixed NP composite on *E. coli* was found to be more effective as compared to the individual components of the composite. Electron microscopic studies revealed that both Cu NPs and Ag NPs were attached to the bacterial cell wall leading to irreversible damage and eventual bacterial death.

Keywords: Chitosan, Copper nanoparticles, Silver nanoparticles, Antimicrobial composite, Bactericidal, Sequential reduction method

Mixed metal nanoparticles (NPs), also called hetero metal NPs, constitute an interesting class of nanomaterials having important applications in several areas of chemistry and physics. The most common application for mixed NPs has been in the area of catalysis where these NPs have been used as catalysts as well as supports for other catalysts[1-4]. The combination of a transition metal element with platinum results in the enhancement of catalytic activities for reactions such as oxygen reduction in fuel cells and direct oxidation of methanol[1]. These studies attracted attention towards preparation of new materials having mixed metal NPs with variable composition displaying unique properties. Various research groups have explored and developed physical and chemical methods for preparing such materials. Bimetallic NPs with core-shell hetero structure or inter-metallic and alloyed structures are being realized as more useful materials than monometallic NPs[5-8].

Phase-separated silver-copper (Ag-Cu) composite colloids containing different mole fractions of Ag and Cu in ethanol solution were synthesized by photo reduction in the presence of benzoin and poly(N-vinyl-2-pyrrolidone) by Itakura *et al*.[9] Suyal *et al*. had synthesized bimetallic alloy and phase separated mixed colloid particles of Cu and Ag in thin films using sol-gel route and studied their optical properties[10]. Woo *et al.* prepared Cu-Ag based mixed metal conductive ink using mixture of Cu NP and Ag NP at varying volume ratios (Cu:Ag) from 2:1 to 4:1 in a mixed solvent system of methanol, 2-methoxy ethanol and ethylene glycol[11]. Li *et al*. developed Ag-Cu colloid ink which they filled into a felt-tip pen and used it to make conducting lines on a substrate[12]. Grouchko *et al*. synthesized well-dispersed Cu NPs by reduction of copper nitrate in aqueous solution using hydrazine monohydrate as a reductant in presence of preformed Ag NPs as catalysts and poly-acrylic acid as a stabilizer[13]. Cu-Ag bimetallic NPs with different hetero structure i.e., alloy, core-shell and heterodimer have been synthesized and their applications studied by several groups. However, *in situ* synthesis of mixed metal NPs in a polymer matrix with emphasis on their biological applications is not well reported.

The antibacterial properties of Cu and Ag, both as bulk and NPs, are well known[14-25]**.** Bactericidal activities of Cu NPs, Ag NPs and their alloy had been reported by our group and others[17,24-26]. Small-sized Cu NPs and Ag NPs (<20 nm diameters) have high bactericidal activity as these NPs get attached to sulphur-containing proteins of bacterial cell membranes altering the permeability of the membrane and causing leakage of proteins and other intracellular material[17,22,23,26]. A few reports have suggested that

Ag^+ and Cu^{2+} ions, generated from the active surfaces of NPs and their oxide present on the surfaces of these NPs, are the actual bactericidal species[15,16,19,27,28]. Recently, chitosan (CS)-supported core-shell Cu@Ag NPs have been prepared and posses excellent antibacterial activity against Gram-negative (*Escherichia coli)* and Gram-positive (*Bacillus cereus*) bacteria[25]. The bactericidal properties of iodinated CS-Ag NP and CS-Cu NPs composite have also been reported[23-25]. Others have demonstrated that Cu-Ag alloy NPs displayed superior bactericidal activity against *E. coli* as compared to pure Ag NPs or Cu NPs[29,30]. Recently M. Valodkar and co-workers had reported preparation of Cu NPs by microwave irradiation using starch as green capping agent. According to their report this biopolymer starch capped Cu NPs are efficient non-cytotoxic bactericidal agents at nanomolar concentrations[31]. However, there is no report about the antibacterial properties of phase separated Cu NPs and Ag NPs working in tandem in the same composite. Herein, the facile preparation of mixed Ag NPs and Cu NPs composites in presence of CS biopolymer and iodine and demonstrate their superior antibacterial activity against *E. Coli* is reported.

Materials and methods

Copper (ll) sulphate pentahydrate ($CuSO_4.5H_2O$), silver nitrate ($AgNO_3$), sodium hydroxide (NaOH, 98%), hydrazine monohydrate (80% solution) and acetic acid (glacial, 99–100%) were procured from Merck (India) and used as received. Milli-Q grade (resistivity 18.2 MΩ cm^{-1}) water was used in all the experiments. Chitosan (high molecular weight, 75% deacetylation) and iodine (I_2) were obtained from Sigma-Aldrich Chemical Pvt. Ltd., Kolkata, India. Luria-Bertani (LB) broth was purchased from HiMedia, Mumbai, India. GFP-expressing recombinant *E. coli* were grown in LB broth at 37 °C in a shaker incubator (at 220 rpm) for 12 h.

Preparation of iodinated CS-supported mixed NP (I_2-CS-Ag NP-Cu NP) composites

Mixed Cu NPs and Ag NPs composite in presence of CS and molecular iodine (abbreviated as I_2-CS-Ag NP-Cu NP composite) by varying the Cu:Ag ratio (Table 1) in a two step reduction process. First, Ag NPs were synthesized by adding the requisite amount of freshly prepared 20 mM $AgNO_3$ solution to 50 mg of chitosan in 50 mL Milli-Q grade water in a 100 mL round bottom flask placed in an oil bath, with vigorous stirring and refluxing for 15 min at ~100 ºC. Then 200 µL of 0.6 M NaOH solution was added to the reaction mixture and within 1 min the solution turned yellow, indicating the formation of Ag NPs in the medium. The reaction was allowed to continue for another 15 min to ensure complete reduction of $AgNO_3$. To this CS-Ag NP dispersion, 40 mg of $CuSO_4.5H_2O$ was added and after 5 min, 0.4 mL of 0.6 M NaOH solution was added upon which the yellow coloured solution turned brown. After 10 min, 0.4 mL of hydrazine monohydrate solution was added to the above solution with constant and vigorous stirring. The reaction was allowed to continue for an additional 30 min until a reddish coloured solid appeared at the bottom of the flask. The flask was then taken out from the oil bath and cooled to room temperature. The solution along with the precipitate was centrifuged at 5300 rpm and the precipitate was washed several times with Milli-Q water and made into a pellet. After complete removal of hydrazine, the pellet was then re-dispersed in 30 mL of 0.25% aqueous acetic acid solution and to this, 0.3 mL of ethanolic iodine solution (0.02 M) was added and mixed thoroughly. UV-visible spectra were recorded for all I_2-CS-Ag NP-Cu NP dispersed solutions. For further characterization of the I_2-CS-Ag NP-Cu NP composites, the reddish solution was centrifuged, vacuum dried and stored under vacuum before analysis.

Characterization of the I_2-CS-Ag NP-Cu NP composites

UV-visible spectra of the I_2-CS-Ag NP-Cu NP composite dispersions were recorded in a Hitachi U2900 spectrophotometer. Transmission electron microscopy (TEM) was carried out in a JEM 2100, machine (JEOL, Peabody, MA,), operating at a maximum accelerating voltage of 200 keV. For this, 5 µL of I_2-CS-Ag NP-Cu NP composite sample was drop-coated onto a carbon coated copper TEM grid followed by air drying. Powder X-ray diffraction (XRD) experiments were carried out using Philips diffractometer (Model 1715) with Cu-Kα1 radiation

Table 1 — Composition used for synthesis of I_2-CS-Ag NP-Cu NP composite

Composites	$CuSO_4.5H_2O$	$AgNO_3$ solution (20 mM)	Cu:Ag molar feed ratio
a	40 mg	600 µL	13.33:1
b	40 mg	400 µL	20:1
c	30 mg	400 µL	15:1
d	20 mg	400 µL	10:1
e	40 mg	200 µL	40:1

(λ = 1.54060 Å), operating at 55 kV and 250 mA. Field emission scanning electron microscopy (FESEM, Carl Zeiss, and Sigma VP) coupled with EDX instruments were used for the study of surface morphology and elemental analysis for I_2-CS-Ag NP-Cu NP composite and composite treated samples. Typically, 10 µL of sample was deposited on a glass slide, dried, sputter-coated with gold film (SC7620 Mini, Polaron Sputter Coater, Quorum Technologies, England) and imaged under the SEM and FESEM. The zeta potential of I_2-CS-Ag NP-Cu NP composites was measured using Delsa TM Nano C particle analyzer (Beckman Coulter®, USA). Fourier transform infrared (FTIR) spectroscopic characterizations of CS and I_2-CS-Ag NP-Cu NPs were carried out in a Perkin-Elmer Spectrum One spectrometer by forming pellets with KBr. Concentrations of Cu and Ag present in I_2-CS-Ag NP-Cu NP composite were measured by atomic absorption spectrophotometer (Model: AA240 Varian Inc) after dissolving the composite in dilute HCl solution. The supernatant solution obtained after centrifugation of the composites was also measured for concentrations of Cu and Ag ions present to determine amount of metal ions being discarded during synthesis.

Bactericidal Studies

Bactericidal studies were carried out on gram negative GFP-expressing *E. coli* bacteria cultured in LB ampicillin media. GFP-expressing *E. coli* (10^8 cfu/mL) were grown in LB media in the presence of different concentrations of I_2-CS-Ag NP-Cu NP for 12 h at 37 ºC. The lowest concentration of composite at which there was no visual turbidity was taken as the minimum inhibitory concentration (MIC) of the composite. Further, the cultures which lacked visual turbidity were re-inoculated in fresh media. The lowest concentration of the composite that killed at least 99.9% of original inoculums was taken as minimum bactericidal concentration (MBC). The experiments were performed in triplicate to ensure reproducibility. The bacterial growth was monitored by measuring optical density (OD) at 595 nm of the sample at different times using a UV-visible spectrophotometer (Lambda-25; Perkin-Elmer, Fremont, CA, USA).

Results and discussion

Synthesis and characterization of I_2-CS-Ag NP-Cu NP composites

The I_2-CS-Ag NP-Cu NP composites were prepared under normal atmospheric conditions. Following the formation of Ag NPs using CS as a reducing and stabilizing agent, Cu NPs were prepared from copper sulfate using hydrazine hydrate as the reducing agent in presence of CS-Ag NPs dispersion. Finally, the I_2-CS-Ag NP-Cu NP composites were formed by adding ethanolic iodine to the CS-Ag NP-Cu NP dispersion. The UV-vis spectrum of a typical I_2-CS-Ag NP-Cu NP composite consisted of two sharp peaks around 415 nm and 585 nm, indicating the formation of Ag NPs and Cu NPs, respectively (Fig. 1). The exact peak positions of the SPR bands due to Ag NPs and Cu NPs varied depending on the Cu:Ag molar feed ratio. The absorption maxima of SPR band due to Ag NPs varied from 400 nm to 415 nm, while that of Cu NPs varied in the range of 575–590 nm. The UV-vis spectra were consistent with the presence of mixed colloids of Ag and Cu NPs in the composite. As the particles were phase separated, their respective plasmon bands were unaffected by the presence of other metal NPs. Thus, the absorption spectrum of I_2-CS-Ag NP-Cu NP composite was a simple addition of the spectra due to Ag NPs and Cu NPs[10]. This also confirmed that Cu and Ag did not form alloys because the UV-vis spectra did not show single peaks positioned in between the individual SPR bands of Ag NPs and Cu NPs, as expected for the Au-Cu and Au-Ag systems[31-33]. It may be mentioned here that stability of the I_2-CS-Ag NP-Cu NP composite depended on Cu:Ag molar feed ratio and was higher at Cu:Ag molar feed ratios of 13.33:1 and 20:1 as compared to that of 10:1 and 40:1 (Supplementary Data, Fig. S1).

TEM analysis of the I_2-CS-Ag NP-Cu NP composites confirmed the presence of metal NPs in all

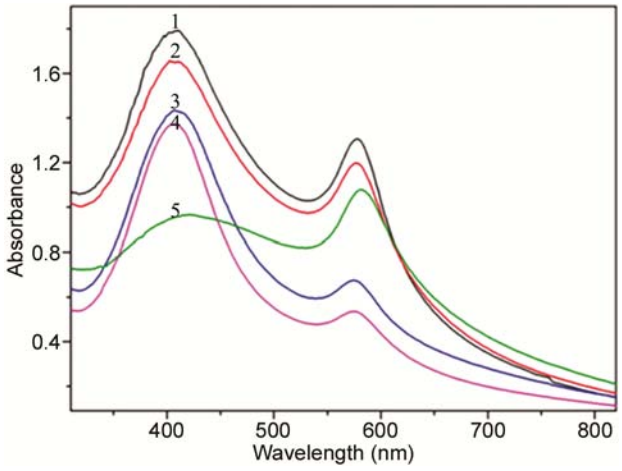

Fig. 1 — UV-visible spectra of freshly prepared I_2-CS-Ag NP-Cu NP composites with Cu:Ag molar feed ratio of (1)13.33:1, (2) 20:1, (3) 15:1, (4) 10:1, and, (5) 40:1.

the cases. The TEM image of I_2-CS-Ag NP-Cu NP composite with Ag:Cu of 13.33:1 is shown in Fig. 2a and the selected area electron diffraction (SAED) patterns of corresponding metal NPs are depicted in Fig. 2b. The indexing of the diffraction rings in Fig. 2b and subsequent determination of the lattice planes (Supplementary Data, Table S1) confirmed the presence of Cu NPs and Ag NPs in face-centered cubic (fcc) lattice structure within the composite. The EDX analysis, carried out on small area of the sample, indicated the presence of the elemental Cu and Ag and I (Supplementary Data, Fig. S2). The XRD pattern of the I_2-CS-Ag NP-Cu NP composite (Ag:Cu of 13.33:1) also indicated the presence of two sets of diffraction peaks which could be assigned to the fcc crystal structure of Cu and Ag (Fig. 2d). The diffraction peaks at 2θ values of 43°, 50°, 74° were due to (111), (200), and (220) planes of fcc Cu(0) (JCPDS-04-0836). The diffraction peaks at 2θ values of 38°, 44°, 64°, 77° and 81° could be assigned to reflections from (111), (200), (220), (331), (222) planes of metallic Ag(0) in fcc structure (JCPDS-04-0783). Appearance of the diffraction pattern was equivalent to simple addition of the corresponding XRD patterns of Cu(0) and Ag(0), which also supported the presence of mixed Cu NPs and Ag NPs[10] . Other I_2-CS-Ag NP-Cu NP composites also produced similar XRD pattern (Supplementary Data, Fig. S3). The presence of CS in the composite was confirmed by FTIR studies (Supplementary Data, Fig. S4).

Furthermore, the I_2-CS-Ag NP-Cu NP composite with Cu:Ag molar feed ratio 20:1 was analyzed under TEM to determine the size distributions of Cu NPs and Ag NPs, as the same composite was chosen for in-depth antibacterial studies (discussed below). The

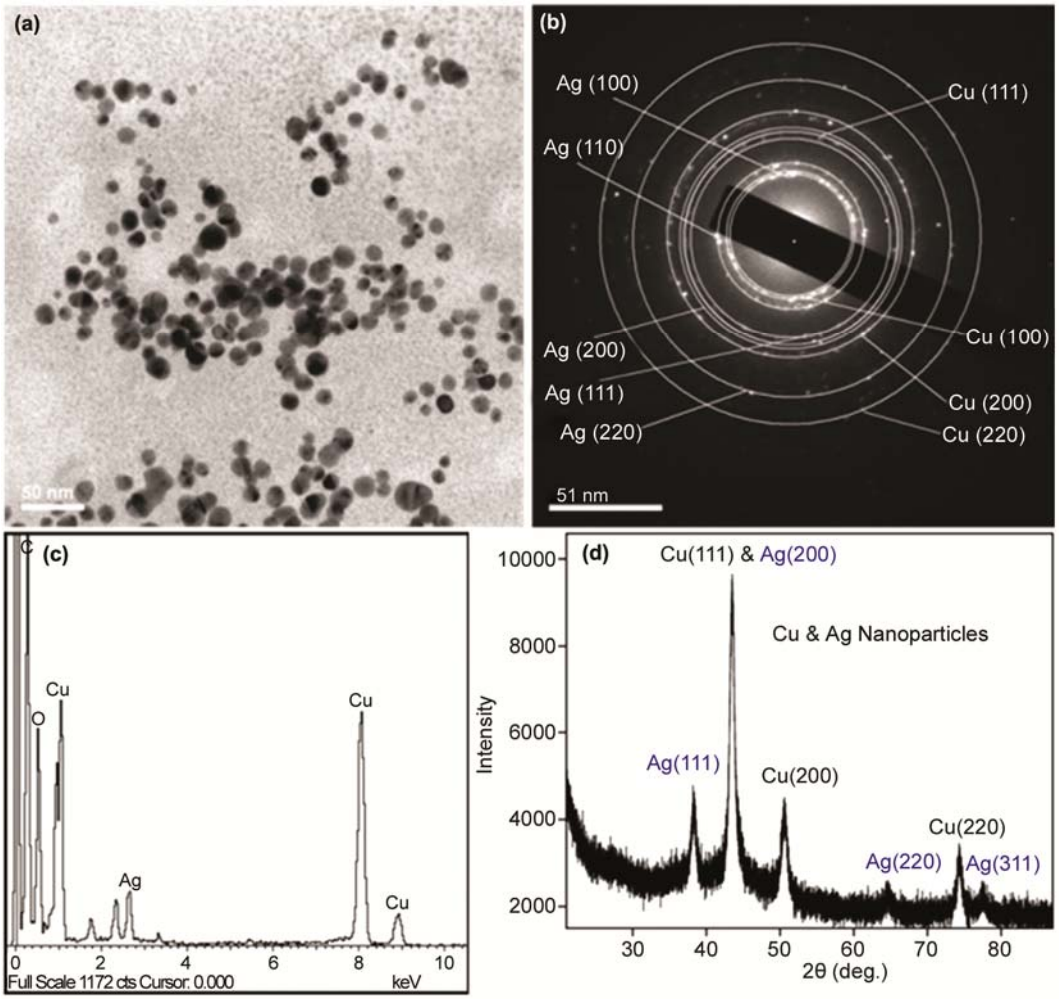

Fig. 2 — TEM micrograph of I_2-CS-Ag NP-Cu NP composite (Cu:Ag molar feed ratio 13.33:1), (b) SAED pattern with the diffraction rings indexed of selected region, (c) EDX profile of I_2-CS-Ag NP-Cu NP composite showing the presence of Cu and Ag, and, (d) XRD pattern of freshly prepared I_2-CS-Ag NP-Cu NP composite (Cu:Ag of 13.33:1).

TEM image of the composite (Cu:Ag molar feed ratio 20:1) is shown in Fig. 3a, while the HRTEM images of corresponding Cu NP and Ag NP are shown in Fig. 3c and Fig. 3d, respectively. The individual Cu NPs as well as Ag NPs were identified based on their corresponding lattice spacings estimated from the inverse Fourier transform (IFFT) of the selected areas of the HRTEM images. The size distribution of Cu NPs and Ag NPs, thus calculated, is shown in Fig. 3b. The Ag NPs (represented by red histogram) was found to have an average size of 3.4±0.9 nm in diameter, while Cu NPs (represented by black histogram) showed an average size of 11.4±3.0 nm in diameter. As was evident from the TEM and HRTEM images in Fig. 3a, both Cu NPs and Ag NPs were found to co-exist in the composite as individual NPs. Also, the IFFT of the HRTEM images (Fig. 3c&d) confirmed that both Cu NP and Ag NP were present in fcc crystal structure with lattice spacing of 0.21 nm and 0.23 nm due to (111) planes of Cu(0) and Ag(0), respectively.

Assessment of antibacterial activity

The bactericidal efficacy of the I_2-CS-Ag NP-Cu NP composites was studied on gram negative GFP-expressing *E. coli* bacteria, a well-established model system to study the antibacterial activities of nanomaterial[17,20,23-25]. GFP-expressing *E. coli* (10^8 cfu/mL) were grown in LB media in the presence of different concentrations of I_2-CS-Ag NP-Cu NP composite (with varying Cu:Ag molar feed ratio) for 12 h. The MIC and MBC values of different I_2-CS-Ag NP-Cu NP composites with corresponding amount of Cu, Ag, CS and I_2 is given in Table 2.

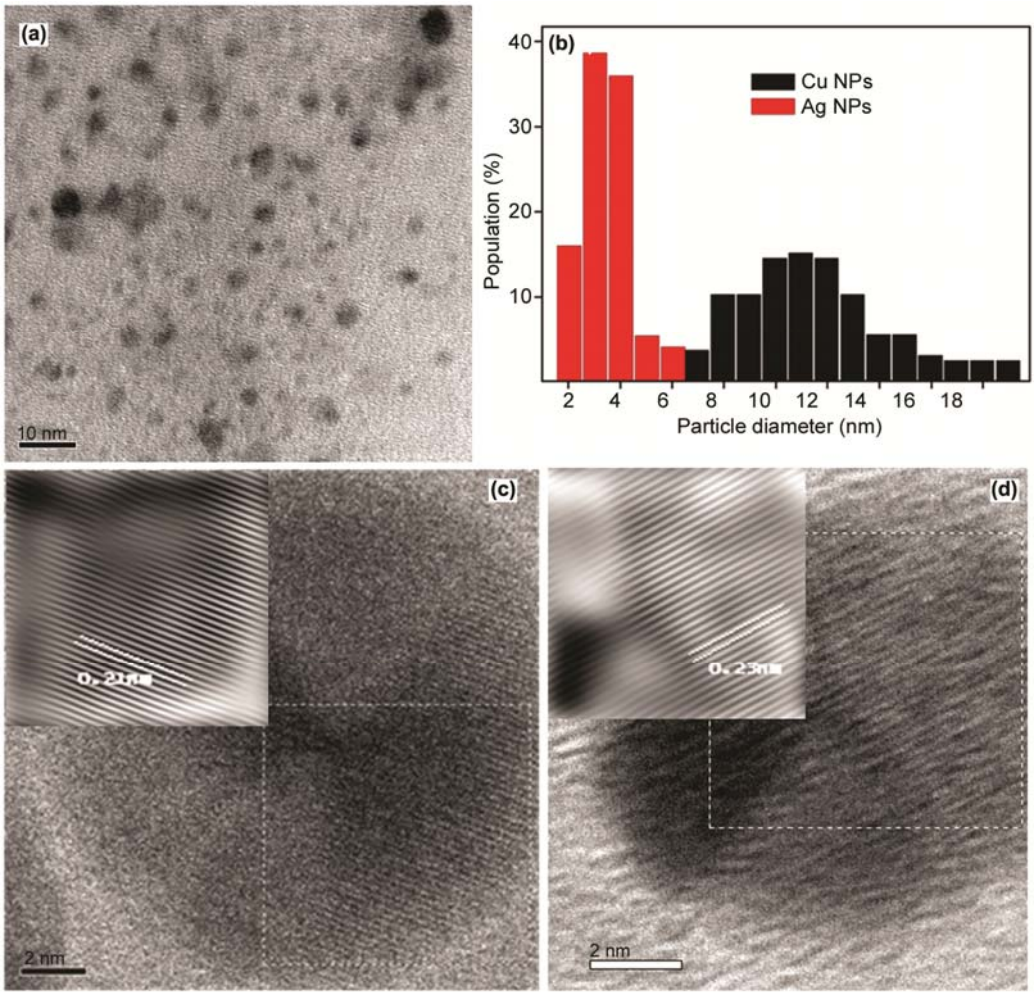

Fig. 3 — (a) TEM image of freshly prepared I_2-CS-Ag NP-Cu NP composite (Cu:Ag molar feed ratios 20:1), (b) size distribution Cu NPs and Ag NPs in the I_2-CS-Ag NP-Cu NP composite, average Ag NPs size 3.4±0.9 nm and Cu NPs size 11.4±3.0 nm, (c) HRTEM image of a particle showing the lattice fringes corresponding to the (111) planes of Cu, [inset: inverse Fourier transform of selected region showing lattice fringes corresponding to the (111) planes of Cu], and, (d) HRTEM image of Ag NP in I_2-CS-Ag NP-Cu NP composite [inset: inverse fourier transform (IFFT) of selected region indicating lattice fringes corresponding to Ag (111) planes].

Table 2 — Antibacterial efficacies of the I_2-CS-Ag NP-Cu NP composites against GFP-expressing *E. coli* bacteria

Cu:Ag molar feed ratio in the composite		Composite (μg/mL)	Cu (μg/mL)	Ag (μg/mL)	CS (μg/mL)	I_2 (μg/mL)
Cu:Ag = 13.33:1	MIC	51.28	8.00	0.95	42.20	0.13
	MBC	75.47	11.27	1.40	62.10	0.19
Cu:Ag = 20:1	MIC	63.50	9.98	0.74	52.64	0.16
	MBC	93.02	14.61	1.08	73.43	0.22
Cu:Ag = 15:1	MIC	81.12	9.73	0.98	70.20	0.21
	MBC	107.58	12.90	1.31	93.08	0.28
Cu:Ag = 40:1	MIC	98.76	15.6	0.44	82.27	0.25
	MBC	132.13	20.86	0.60	110.07	0.33

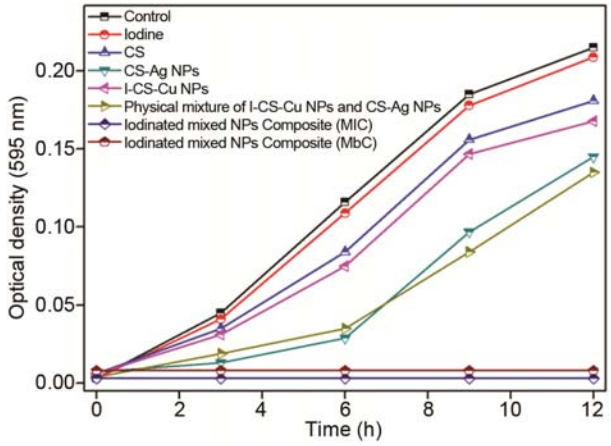

Fig. 4 — Growth curve of GFP recombinant *E. coli* in the presence of Control (0.02 M acetic acid and 6 μL ethanol), Iodine (iodine, 0.16 μg/mL), CS (chitosan, 52.64 μg/mL), CS-Ag NPs (CS-Ag NP composite, 53.40 μg/mL), I-CS-Cu NPs (iodinated CS-Cu NP composite, 63.20 μg/mL), Physical mixture of I-CS-Cu NPs and CS-Ag NPs (1:1 *v*/*v*; amounts of components in mixed solution: CS 52.0 μg/mL, Ag 0.73 μg/mL, Cu 5.0 μg/mL, I_2 0.08 μg/mL), Iodinated mixed NPs Composite (MIC) (I_2-CS-Ag NP-Cu NP composite, 63.50 μg/mL) and Iodinated mixed NPs Composite (MBC) (I_2-CS-Ag NP-Cu NP composite, 93.02 μg/mL).

The I_2-CS-Ag NP-Cu NP composite with Cu:Ag molar feed ratio of 20:1 was chosen for further antibacterial studies because of its improved stability and bactericidal activity at low concentration of Cu and Ag. It may be mentioned here that the MIC of this I_2-CS-Ag NP-Cu NP composite (Cu:Ag = 20:1) was found to be 63.50 μg/mL which consisted of 9.98 μg/mL of Cu NPs and 0.74 μg/mL of Ag NPs. The corresponding MBC (93.02 μg/mL) contained 14.61 μg/mL Cu NP and 1.06 μg/mL of Ag NPs. In order to gain insight into the bactericidal action, bacterial growth in presence of I_2-CS-Ag NP-Cu NP composite at MIC and MBC was investigated. Appropriate experiments were also carried out for the comparison of antibacterial efficacies of individual components of the final I_2-CS-Ag NP-Cu NP composite. As evident from Fig. 4, control samples showed no growth inhibition. The individual components (at their respective concentrations in the composite) either did not exhibit antibacterial properties (such as 0.16μg/mL of iodine) or exhibited limited bactericidal properties [such as 52.64 μg/mL of CS; 53.40 μg/mL of CS-Ag NP composite (CS:Ag = 1:0.17); 63.20 μg/mL of iodinated CS-Cu NP composite (CS:Cu:I = 1:0.20:0.003)]. Interestingly, a physical mixture of I-CS-Cu NPs and CS-Ag NPs (1:1 *v*/*v*) which consisted CS 52.0 μg/mL, Ag 0.73 μg/mL, Cu 5.0 μg/mL, I_2 0.08 μg/mL exhibited limited bactericidal properties. The result clearly demonstrated the superior antibacterial efficacy of I_2-CS-Ag NP-Cu NP composite system as compared to individual components at their individual concentrations in the composite. This could be due to the smaller Ag NPs and Cu NPs working in tandem with CS and iodine within the composite resulting in heightened bactericidal activity.

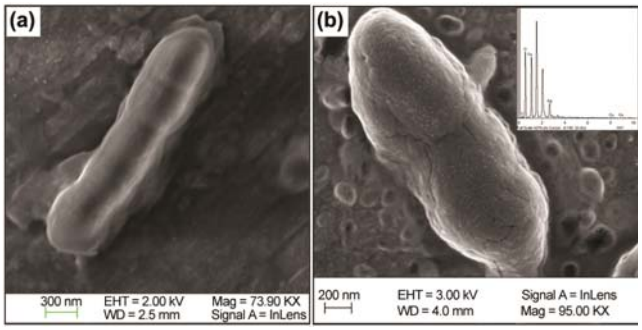

Fig. 5 — FESEM image of GFP expressing recombinant *E. coli* cells in (a) non-treated sample and (b) sample treated with I_2-CS-Ag NP-Cu NP composite (63.50 μg/mL) for 4 h [inset: FESEM-EDX profile indicating presence of elemental Cu and Ag in corresponding sample].

Interaction of the I_2-CS-Ag NP-Cu NP composite (Cu:Ag of 20:1) with *E. coli* was investigated under TEM and FESEM, after treating the bacteria with MIC dose of composite for 4 h. The FESEM images of untreated and composite-treated GFP recombinant *E. coli* are shown in Fig. 5. While the untreated

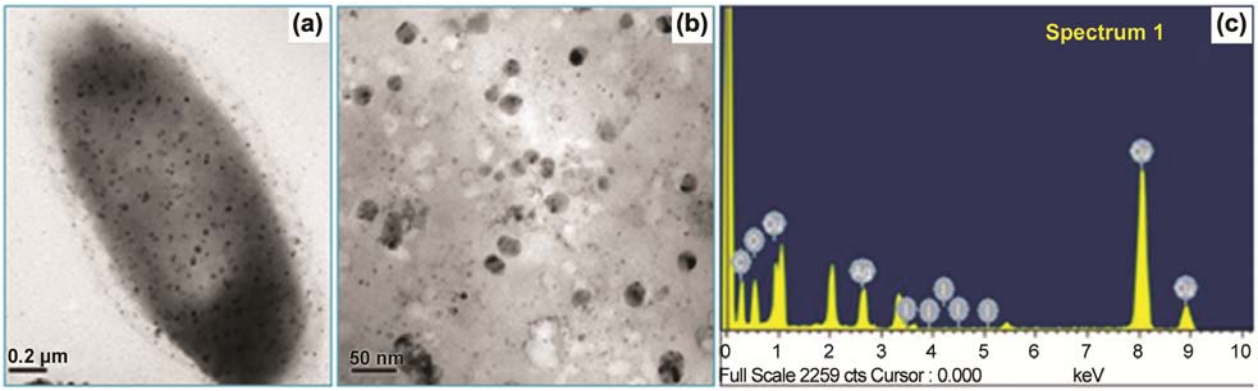

Fig. 6 — Transmission electron micrograph of GFP expressing recombinant *E. coli* cells treated with 63.50 µg/mL (MIC) I_2-CS-Ag NP-Cu NP composite in liquid LB medium for 4 h. TEM micrograph show both Cu NPs (12±3.0 nm) and Ag NPs (3.5±1nm) interacting with *E. coli* cells. TEM-EDX profiles also show presence of elemental Cu and Ag and iodine of composite treated samples.

control bacteria showed normal surface morphology (Fig. 5a), the treated bacteria were observed to be distinctly different with the bacterial cells covered with a layer of the composite (Fig. 5b). In the presence of I_2-CS-Ag NP-Cu NP composite, the positively charged CS could readily attach to the negatively charged bacterial cell wall[23-25]. The zeta potential values of various I_2-CS-Ag NP-Cu NP composite (+35 mV for composite with Cu:Ag of 20:1), (Supplementary Data, Table S2), also indicated towards the potential electrostatic interaction between the I_2-CS-Ag NP-Cu NP composite and bacterial cell wall. Chitosan (a β-1,4 linked glucosamine) is a known biopolymer possessing bactericidal activity against gram-negative and gram-positive bacteria. CS interacts with bacterial cell wall through electrostatic attractions as CS is polycationic in nature and the bacterial cell envelop is negatively charged[23-25]. Herein, positively charged CS facilitates the attachment of Cu NPs, Ag NPs along with composite to the bacterial cell wall through electrostatic interactions.

On the other hand, the TEM image of treated bacteria (Fig. 6a&b) clearly showed the presence of small spherical NPs over the cell surface. Small metal NPs with diameter of 13.5± 3.5 nm for Cu NPs and diameter of 4.2 ±1.0 nm for Ag NPs were clearly discernible (Supplementary Data, Fig. S5). That these two size distributions were very similar to those of Cu NPs and Ag NPs in the original I_2-CS-Ag NP-Cu NP composite (Fig. 3b), corroborates well with the conclusion that Ag and Cu NPs got attached to the bacterial cell wall causing irreparable damage (Fig. 6a&b). Similar results were also observed in previous studies for CS-stabilized Cu NPs (~15 nm) and CS-stabilized Ag NPs (~10 nm), where the metal NPs were found to interact with the bacterial cell wall inducing pore formation and leading to death of the bacteria[23-25]. Moreover, the EDX profile of the treated bacterial sample, shown in Fig. 6c, confirmed the presence of Cu, Ag and iodine in the composite attached to the bacteria.

Conclusions

A novel method for preparing bimetallic mixed NPs composites comprising Ag NPs and Cu NPs in CS matrix along with molecular iodine has been developed. Following complete physicochemical characterization, the I_2-CS-Ag NP-Cu NP composite was evaluated for their potential antibacterial activity on GFP-expressing *E. coli* bacteria. The results demonstrated the superior bactericidal properties of the I_2-CS-Ag NP-Cu NP composites as compared to the individual components. The electron microscopic analysis revealed that the I_2-CS-Ag NP-Cu NP composite interacted with the bacterial cell wall leading to the destabilization of its integrity. The combination of Ag NPs and Cu NPs with natural biopolymers CS and molecular iodine enhanced bactericidal efficiency as CS attached to the bacterial cell wall while the metal NPs in the composite turned the cell wall porous. Additionally, the molecular iodine upon dissociation from the metallic surfaces led to the enhancement of antibacterial activity, resulting in the death of bacteria at very low doses of each component.

Supplementary data

Supplementary data associated with this article are available in the electronic form at http://www.niscair.res.in/jinfo/ijca/IJCA_57A(10)1249-1256_SupplData.pdf.

Acknowledgement

Department of Science and Technology (DST), Department of Biotechnology (DBT), and Council of Scientific and Industrial Research (CSIR) are acknowledged for funds. The author also thanks CSIR for a fellowship (09/731(0061)/2008-EMR-I). Assistance from Central instruments facility (CIF), Department of Physics for DST-FIST X-ray Diffractometer, New Delhi, (ref no : SR/FST/PS11-020/2009) is gratefully acknowledged. Bruker AXS D8 Advance X-ray diffractometer facility, and Centre for the Environment for atomic absorption spectroscopic studies at IIT Guwahati are gratefully acknowledged.

References

1 Zhang X & Chan K Y, *J Mater Chem*, 12 (2002) 1203.
2 Zhang X & Chan K Y, *Chem Mater*, 15 (2003) 451.
3 Liu Z, Lee J Y, Han M, Chen W & Gan L M, *J Mater Chem*, 12 (2002) 2453.
4 Zeng J & Lee J Y, *Mater Chem Phys*, 104 (2007) 336.
5 Harpeness R & Gedanken A, *Langmuir*, 20 (2004) 3431.
6 Lim B, Kobayashi H & Yu T, *J Am Chem Soc*, 132 (2010) 2506.
7 Butovsky E, Perelshtein I & Gedanken A, *J Mater Chem*, 22 (2012) 15025.
8 Huang X, Li Y, Zhou H, Zhong X, Duan X & Huang Y, *Chem Eur J*, 18 (2012) 9505.
9 Itakura T, Torigoe K & Esumi K, *Langmuir*, 11 (1995) 4129.
10 Suyal G, *Thin Solid Films*, 426 (2003) 53.
11 Woo K, Kim D, Kim J S, Lim S & Moon J, *Langmuir*, 25 (2008) 429.
12 Li Y S, Lu Y C, Chou K S & Liu F J, *Mater Res Bull*, 45 (2010) 1837.
13 Grouchko M, Kamyshny A, Ben-Ami K & Magdassi S, *J Nanopart Res*, 11 (2009) 713.
14 McLean R J, Hussain A A, Sayer M, Vincent P J, Hughes D J & Smith T J, *Can J Microbiol*, 39 (1993) 895.
15 Feng Q L, Wu J, Chen G Q, Cui F Z, Kim T N & Kim J O, *J Biomed Mater Res*, 52 (2001) 662.
16 Morones J R, Elechiguerra J L, Camacho A, Holt K, Kouri J B, Ramírez J T & Yacaman M J, *Nanotechnol*, 16 (2005) 2346.
17 Gogoi S K, Gopinath P, Paul A, Ramesh A, Ghosh S S & Chattopadhyay A, *Langmuir*, 22 (2006) 9322.
18 Pal S, Tak Y K & Song J M, *Appl Environ Microbiol*, 73 (2007) 1712.
19 Yoon K Y, Byeon J H, Park J H & Hwang J, *Sci Total Environ*, 373 (2007) 572.
20 Sanpui P, Murugadoss A, Prasad P D, Ghosh S S & Chattopadhyay A, *Int J Food Microbiol*, 124 (2008) 142.
21 Ruparelia J P, Chatterjee A K, Duttagupta S P & Mukherji S, *Acta Biomater*, 4 (2008) 707.
22 Wei Y, Chen S, Kowalczyk B, Huda S, Gray T P & Grzybowski B A, *J Phys Chem C*, 114 (2010) 15612.
23 Banerjee M, Mallick S, Paul A, Chattopadhyay A & Ghosh S S, *Langmuir*, 26 (2010) 5901.
24 Mallick S, Sharma S, Banerjee M, Ghosh S S, Chattopadhyay A & Paul A, *ACS Appl Mater Interfaces*, 4 (2012) 1313.
25 Mallick S, Sanpui P, Ghosh S S, Chattopadhyay A & Paul A, *RSC Adv*, 5 (2015) 12268.
26 Sondi I & Salopek-Sondi B, *J Colloid Interface Sci*, 275 (2004) 177.
27 Borkow G & Gabbay J, *Curr Med Chem,* 12 (2005) 2163.
28 Cioffi N, Ditaranto N, Torsi L, Picca R A, Giglio E De, Sabbatini L, Novello L, Tantillo G, Bleve-Zacheo T P & Zambonin G, *Anal Bioanal Chem*, 382 (2005) 1912.
29 Valodkar M, Modi S, Pal A & Thakore S, *Mater Res Bull*, 46 (2011) 384.
30 Taner M, Sayar N, Yulug I G & Suzer S, *J Mater Chem*, 21 (2011) 13150.
31 Valodkar M, Rathore P S, Jadeja R N, Thounaojam M D, Ranjitsinh V & Thakore S, *J Hazard Mater*, 201 (2012) 244.
32 Smetana A B, Klabunde K J, Sorensen C M, Ponce A A & Mwale B, *J Phys Chem B*, 110 (2006) 2155.
33 Chowdhury S, Bhethanabotla V R & Sen R, *Appl Phys Lett*, 95 (2009) 131115.
34 Tabrizi N S, Xu Q, van der Pers, N M & Schmidt-Ott A, *J Nano Res*, 12 (2010) 247.